

## Supplemental Tables

**Table S1.** Data collection and refinement statistics for the RNF4 RING domain structure.

		RNF4		
<b>Data collection</b>				
Space group		<i>P2<sub>1</sub>2<sub>1</sub>2</i>		
Cell dimensions				
<i>a, b, c</i> (Å)		58.56, 86.10, 22.25		
$\alpha, \beta, \gamma$ (°)		90, 90, 90		
	Peak	Inflection	Remote	
Wavelength (Å)	1.2829	1.2833	1.2523	
Resolution (Å)	19.51-1.80 (2.84-2.54)	19.51-1.80 (2.84-2.54)	19.51-1.80 (1.89-1.80)	
<i>R</i> <sub>merge</sub>	9.5 (19.4)	9.6 (21.7)	6.9 (27.4)	
<i>I</i> / $\sigma$ <i>I</i>	14.0 (7.8)	13.8 (8.1)	15.3 (6.0)	
Completeness (%)	99.1 (97.9)	98.8 (97.3)	99.1 (98.8)	
Redundancy	6.4 (6.6)	6.4 (6.5)	6.6 (6.5)	
<b>Refinement</b>				
Resolution (Å)		18.73-1.80		
No. reflections		10349		
<i>R</i> <sub>work</sub> / <i>R</i> <sub>free</sub>		18.73/24.20		
No. atoms				
Protein		1038		
Ligand/ion		4		
Water		43		
<i>B</i> -factors				
Protein		23.59		
Ligand/ion		14.79		
Water		33.70		
R.m.s. deviations				
Bond lengths (Å)		0.01		
Bond angles (°)		1.50		

Values in parentheses are for highest-resolution shell.

## Supplementary Figures

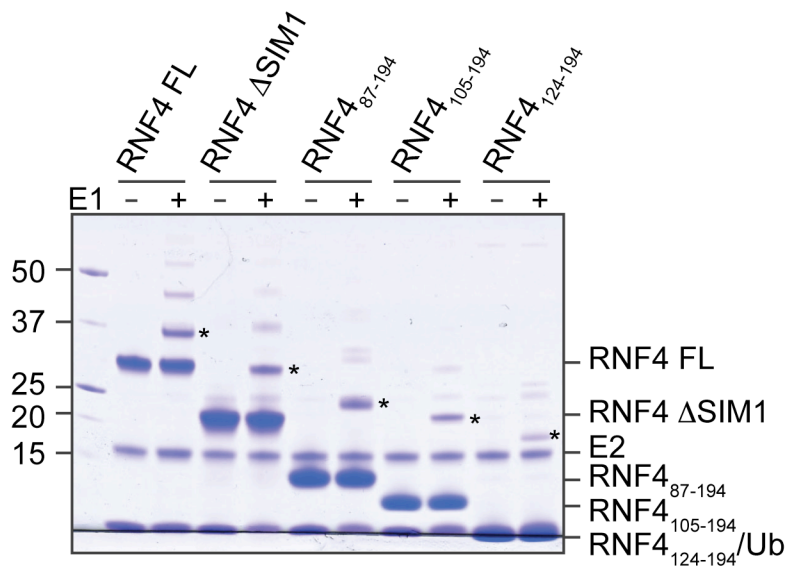


**Figure S1.** Autoubiquitylation assays showing the E3 ligase activity of RNF4 constructs. Reactions were incubated at 37°C for 90 minutes in the presence or absence of E1 as indicated. Mono-ubiquitylated species are indicated by an asterisk. Note that ubiquitin and RNF4 RING (residues 124-194) run on top of each other.

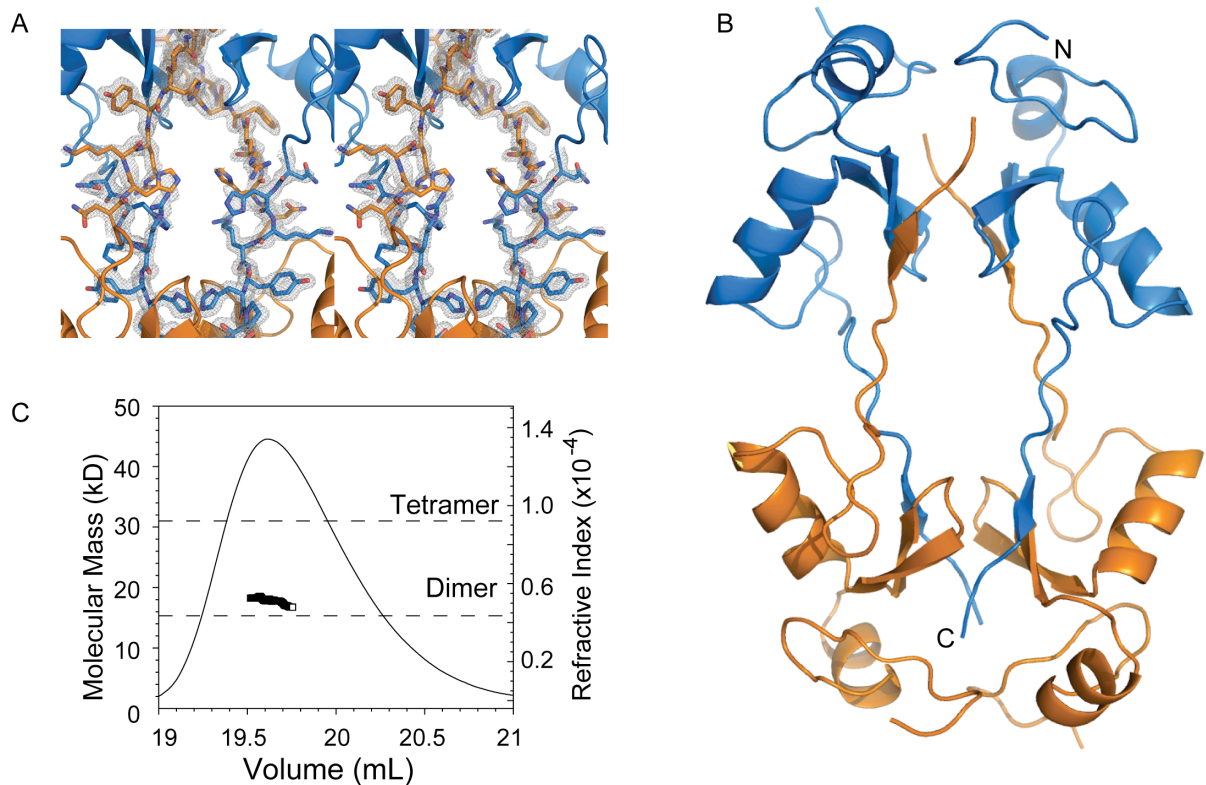


**Figure S2.** (A) Stereo view of a partial electron density map contoured at  $1\sigma$  showing domain swapping of the RNF4 RING domain C-terminal tails. (B) Ribbon diagram of RNF4 showing the domain swapped tetramer. (C) A sample of the RNF4 RING domain at 0.6 mM was separated in 1xPBS on a Superdex S200 column that was coupled to a MALLS detector. The refractive index profile and the calculated mass are shown. The horizontal lines indicate the expected mass of the tetramer and dimer.

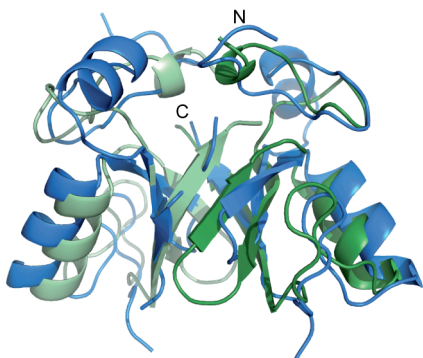


**Figure S3.** RNF4 adopts a typical RING-domain fold (blue) and overlays closely to the MDM2:MDMX heterodimer (MDM2 in dark green and MDMX in light green) (PDB 2VJE).

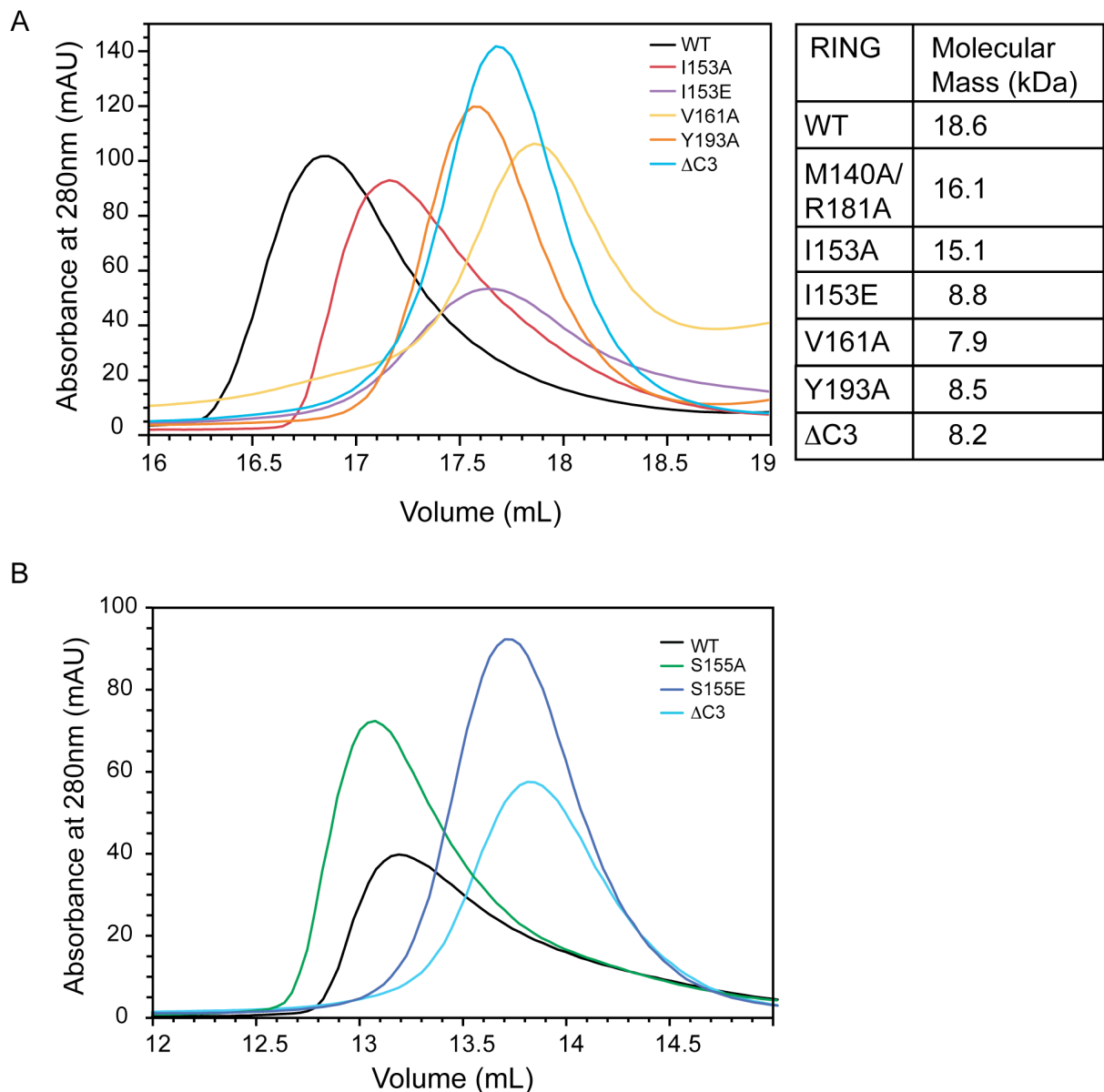


**Figure S4.** (A) Elution profiles of additional RNF4 RING domain mutants and corresponding molecular masses determined by MALLS analysis. The elution profiles of wild type (WT), I153A and  $\Delta$ C3 are shown for reference. Samples of the RNF4 RING domain at  $\sim$ 0.3-0.5 mM were separated in 1xPBS on a Superdex S200 column that was coupled to a MALLS detector. The M140A/R181A mutant was separated on a S75 column connected to the MALLS detector and the trace is not shown. (B) Elution profiles of S155A and S155E together with the dimeric wild type and monomeric  $\Delta$ C3. Samples of the RNF4 RING domain at  $\sim$ 40-70  $\mu$ M were separated in 1xPBS on a Superdex S75 column.

## Supplementary Methods

### *Crystallization and structure solution*

Following collection of data at beamline PX-2 at the Australian Synchrotron data were integrated using the program package xds (Kabsch, 1993). Scaling and processing were carried out using the CCP4 V6.1.1 program suite (CCP4, 1994). Phase calculation was carried out using the autoSHARP software interface. Four zinc atom sites were located using SHELXD (Schneider and Sheldrick, 2002). Solvent flattening was carried out in SOLOMON (Abrahams and Leslie, 1996) resulting in electron density maps that were of sufficient quality to allow manual building of an initial model using COOT (Emsley and Cowtan, 2004). The initial model was refined against the remote dataset using REFMAC V5.5.0072 (Murshudov et al 1999), followed by iterative cycles of manual model rebuilding and refinement using a weighting of 0.3 between X-ray and geometry terms as well as NCS restraints. Data processing and final refinement statistics are presented in Table 1. Interface analysis was carried out with PISA at the EBI website (Krissinel and Henrick, 2005) and structure figures were generated using PyMOL (DeLano, 2002).

### **Supplementary References**

- Abrahams, J. P. & Leslie, A. G. (1996) Methods used in the structure determination of bovine mitochondrial F1 ATPase. *Acta Crystallogr D Biol Crystallogr* **52**, 30-42.
- CCP4. (1994) The CCP4 suite: programs for protein crystallography. *Acta Crystallogr D Biol Crystallogr* **50**, 760-3.
- DeLano, W. L. (2002) *The PyMol Molecular Graphics System*, DeLano Scientific, Palo Alto, CA, USA.
- Emsley, P. & Cowtan, K. (2004) Coot: model-building tools for molecular graphics. *Acta Crystallogr D Biol Crystallogr* **60**, 2126-32.
- Kabsch, W. (1993) Automatic processing of rotation diffraction data from crystals of initially unknown symmetry and cell constants. *Journal of Applied Crystallography* **26**, 795-800.
- Krissinel, E. & Henrick, K. (2007) Inference of macromolecular assemblies from crystalline state. *J Mol Biol* **372**, 774-797
- Murshudov, G. N., Vagin, A. A. & Dodson, E. J. (1997) Refinement of macromolecular structures by the maximum-likelihood method. *Acta Crystallogr D Biol Crystallogr* **53**, 240-255.
- Schneider, T. R. & Sheldrick, G. M. (2002) Substructure solution with SHELXD. *Acta Crystallogr D Biol Crystallogr* **58**, 1772-1779.